Title

Thermal transport in amorphous small organic materials: a mechanistic study

Journal

Physical Chemistry Chemical Physics, 22(5)

ISSN

0956-5000

Authors

Zhou, Tian
Li, Zhuhong
Cheng, Yajuan
et al.

Publication Date

2020-02-07

DOI

10.1039/c9cp05938e

Peer reviewed

Thermal transport in amorphous small organic materials: A mechanistic study

Tian Zhou[1,+], Zhuhong Li[1,+], Yajuan Cheng[2], Yuxiang Ni[3], Sebastian Volz[4], Davide Donadio[5], Shiyun Xiong[1,*], Wenqing Zhang[6], Xiaohong Zhang[1,*]

1. Institute of Functional Nano & Soft Materials (FUNSOM), Jiangsu Key Laboratory for Carbon-Based Functional Materials & Devices, Soochow University, 199 Ren'ai Road, Suzhou, 215123, Jiangsu, P. R. China.
2. Key Laboratory of Organic Synthesis of Jiangsu Province and the State and Local Joint Engineering Laboratory for Novel Functional Polymeric Materials, College of Chemistry, Chemical Engineering and Materials Science, Soochow University, Suzhou 215123, P. R. China.
3. School of Physical Science and Technology, Key Laboratory of Advanced Technologies of Materials, Ministry of Education of China, Southwest Jiaotong University, 610031 Chengdu, P.R. China.
4. LIMMS/CNRS-IIS(UMI2820) Institute of Industrial Science, University of Tokyo 4-6-1 Komaba, Meguro-ku, 153-8505 Tokyo, Japan.
5. Department of Chemistry, University of California Davis, One Shields Ave. Davis, California 95616, United States.
6. Department of Physics, Southern University of Science and Technology, Shenzhen 518055, China
+these authors contribute equally.
Email: **xiongshiyun216@163.com; xiaohong_zhang@suda.edu.cn;**

Abstract

Understanding the thermal transport mechanisms in amorphous organic materials is of great importance to solve hot-spot issues in organic-electronics nanodevices. Here we studied thermal transport in two popular molecular electronic materials, N,N-dicarbazolyl-3,5-benzene (mCP) and N,N'-diphenyl-N,N'-di(3-methylphenyl) -(1,1'-biphenyl)-4,4'diamine (TPD), by molecular dynamics simulations. We found that due to the softness of organic materials, the low thermal conductivity of both systems can be greatly enhanced under pressure. Notably, in such systems, the convective term of the heat flux provides an important contribution to thermal transport as it cross-correlates with the Virial term in the Green-Kubo formula. Mode diffusivity calculations reveal that low-frequency modes can contribute significantly to thermal transport in both mCP and TPD. Increasing the pressure, the sound velocity and relaxation time of such low-frequency modes can be enhanced, and part of these modes convert from *diffusons* to *propagons*. The cooperation of these three effects is responsible for the strong pressure dependence of thermal transport in amorphous organic systems. Molecular pair heat flux calculations demonstrate that heat transfer mainly happens between pairs of molecules with distances below 1.4 nm. This work paves the way to the optimization of thermal transport in amorphous organic materials widely used in opto-electronics, e.g. as OLED and OPV.

1 Introduction

The rapid development of organic electronics has greatly attracted the attention of the electronics industry and research community, including organic photovoltaic devices (OPV), organic field effect transistors (OFET), and organic light emitting diodes (OLED)[1, 2]. Organic electronic devices (OED) often employ materials made of easy to process small organic molecules. Various approaches, such as heat evaporation, solution shearing or vapor phase deposition, were successfully used to fabricate organic electronic devices[3]. During the past decade, OED have been continuously scaled down in size, while the power density has increased dramatically. As a result, heat dissipation has become a critical issue, as it may degrade the performance or even reduce the stability of OED. This problem is aggravated by the low thermal conductivity of (macro)molecular materials. Consequently, the new generation of OED should entail high thermal conductivity (TC) to spread thermal energy efficiently.

Heat transport in inorganic materials has been investigated for a long time and its fundamental microscopic mechanisms are well understood. However, studies of organic materials are much fewer, and, besides carbon nanostructures (carbon nanotubes[4], graphene[5]), most of them have focused on polymers[6]. For example, Tang *et al.*[7] measured thermal transport in polyacrylamide (PAAm) hydrogels and found that their TC could be modulated by the effective crosslinking density, due to the competition between the increased conduction pathways and the enhanced phonon scattering. Shen *et al.*[8] found that the TC of polyethene (PE) can be enhanced by two orders of magnitude by stretching it to fibers, which can be related to the abnormal heat conduction in single PE chain as demonstrated by Henry *et al.*[9] The understanding of thermal transport in crystalline and amorphous molecular materials made of small organic molecules is still incomplete and the transport mechanisms need yet to be clarified. Differing from polymers, small organic molecules, which are the main component of many OED, have much less covalent bonds. Although the thermal transport in some organic molecular crystals, such as pentacene, has been investigated by of non-equilibrium molecular dynamics[3, 10], the transport behavior of amorphous films made of small organic molecules has rarely been studied[11]. However, amorphous molecular materials are widely used in electronic devices, such as OLED. In the amorphous state, the lack of periodicity makes transport more complicated compared to crystalline structures. Moreover, in OED, pressure can be applied to improve the device performance[**JOURNAL OF APPLIED PHYSICS 115, 233703 (2014)**]. While the detailed effect of pressure on thermal transport in amorphous organic materials is still unclear. As a result, it is crucial to study thermal transport and clarify the corresponding mechanisms in amorphous organic molecules.

In this work, we perform molecular dynamics simulations to unravel the thermal transport properties of two typical small organic molecules in their amorphous state, i.e., N,N-dicarbazolyl-3,5-benzene (mCP) and N,N'-diphenyl-N,N'-di(3-methylphenyl) -(1,1'-biphenyl)-4,4'diamine (TPD). The effects of temperature and pressure on TC are investigated and the corresponding molecular mechanisms governing thermal transport is studied in terms of spectral heat current and mode diffusivity.

2 Simulation Details

All simulations are conducted with LAMMPS code[12] with the interatomic interactions described by the OPLS force field[13]. The parameters to model flexible bonds (dihedrals, impropers and

angles associate with two rigid fragments) and atomic charges are fitted from quantum chemistry calculations (See details in supplementary materials). All the parameters used for the force field can be found in the supplementary material. All amorphous structures were constructed by quenching from the melt: All systems are first equilibrated in a molten state at 600 K and 100 Pa with isothermal-isobaric conditions (NPT ensemble[14]) for 2 ns, during which the equilibrium density is achieved. Then, the systems are quenched by ramping the temperature in subsequent NPT simulations at a rate of 60 K/ns, thus equilibrating the density at every temperature. The final length of the cubic simulation box is about 4.6 nm at 300 K and 100 Pa. Periodic boundary conditions are applied in all three directions and a 0.5 fs timestep is chosen so to ensure accurate integration of the equations of motion. For thermal transport calculations, the glassy systems were first equilibrated at isothermal-isobaric conditions at target temperature and pressure for 2.5 ns, during which the density relaxes to the equilibrium value at the corresponding thermodynamic conditions. Eventually, we performed a run in the canonical ensemble (NVT) for 1 ns, during which we extracted 10 structures, one every 100 ps. After that, we perform 5 ns of NVE simulations for each structure and the heat flux is collected every 5 fs during the last 2.5 ns. The TCs were calculated based on the obtained integrating the heat flux correlation function, according to the Green-Kubo formula[15, 16]. The final values were averaged over the values in the three directions of the ten structures, i.e., 30 data sets, and the error bars were calculated as the standard error of these data.

To evaluate the TC based on the Green-Kubo formula, the heat flux should be calculated first. The heat flux at equilibrium is calculated according to the following formula:

$$J = \frac{1}{V}\left[\sum_i e_i \mathbf{v}_i + \frac{1}{2}\sum_{i<j}(\mathbf{F}_{ij}\cdot(\mathbf{v}_i+\mathbf{v}_j))\mathbf{x}_{ij}\right] \quad (1)$$

Where e_i is the total energy of atom i, $\mathbf{v}_i$ and $\mathbf{v}_j$ represent the velocity of atom i and j, respectively. $\mathbf{F}_{ij}$ and $\mathbf{x}_{ij}$ are the force and position vector between atoms i and j, respectively. The first and the second parts of the above equation correspond to the convective and the Virial contribution to the total heat flux. The convective part $\{\sum_i e_i \boldsymbol{v_i}\}$ may provide a substantial contribution to TC in liquid systems but for solids, it does not usually contribute significantly. Hence, this term in Eq. (1) is often neglected when simulating thermal transport in solids. To check the importance of the convective part to the total TC in organic materials, we calculated the TC based on the total heat flux and only the Virial part of the heat flux.

The phonon density of states (DOS) is a quantity that characterizes the distribution of phonon modes of a system quantitatively, thus it can be used to reveal the physics of thermal energy transport. The phonon DOS at frequency ω, $DOS(\omega)$, can be evaluated by taking the Fourier transform of the velocity autocorrelation function (VACF)[17]:

$$DOS(\omega) = \frac{1}{\sqrt{2\pi}}\sum_{i,\alpha}\int_{-\infty}^{\infty} e^{i\omega t}\frac{\left\langle v_i^{\alpha}(t)\cdot v_i^{\alpha}(0)\right\rangle}{\left\langle v_i^{\alpha}(0)\cdot v_i^{\alpha}(0)\right\rangle}\mathrm{d}t \quad (2)$$

where v_i^{α} denotes the velocity of atom i in direction α and t represents the correlation time. In amorphous materials, the mode diffusivity is an important quantity to describe the thermal transport. The mode diffusivity can be casted according to the Allen-Feldman theory [18], where the diffusivity of an individual mode D_i is defined as:

$$D_i = \frac{\pi V^2}{\hbar^2 \omega^2} \sum_{j \neq i} |\langle i | J | j \rangle|^2 \, \delta(\omega_i - \omega_j) \tag{3}$$

Where ω_i and ω_j are the frequency of mode i and j, respectively. V represents the volume of the system. $\langle i|J|j\rangle$ is the heat flux operator projected on the vibrational eigenstates, $\delta(\omega_i - \omega_j)$ is a Lorentzian function with width 0.002 rad/ps that takes into account the broadening of vibrational modes. With the obtained diffusivity, the TC contributed by an individual mode i is casted as:

$$\kappa = \sum_i \kappa_i = \frac{1}{V} \sum_i C_i D_i \tag{4}$$

where C_i denotes the specific heat of the harmonic oscillator, and T is the temperature.

Mode diffusivity can provide a good estimation on the TC contributed by high frequency modes in amorphous materials, where thermal energy is transported through the hopping of modes with similar frequencies, i.e. *diffusons*. However, at low frequencies, the mode mean free path (MFP) is large and cannot be characterized by mode diffusivity. To check the contributions of the low frequency modes, we also calculated the spectral heat current with non-equilibrium molecular dynamics. The spectrally decomposed heat current can be summed over the heat flux $q_{i\to j}(\omega)$ between atoms i and j that respectively belong to adjacent blocks L and R:[19]

$$q(\omega) = \frac{1}{A} \sum_{i \in L} \sum_{i \in R} q_{i \to j}(\omega) \tag{5}$$

Where A is the cross-section and the spectral heat flux $q_{i\to j}(\omega)$ can be calculated as:[20]

$$q_{i \to j}(\omega) \approx -\frac{2}{t_s \omega} \sum_{\alpha,\beta \in \{x,y,z\}} \mathrm{Im} \left\langle \hat{v}_i^{\alpha}(\omega)^* K_{ij}^{\alpha\beta} \hat{v}_i^{\beta}(\omega)^* \right\rangle \tag{6}$$

In this formula t_s refers to the total simulation time, v_i^{α} (v_i^{β}) is the Fourier transformed velocity of atom i in direction α (β) belonging to x, y, and z. $K_{ij}^{\alpha\beta}$ represents the force constant associating atom i in direction α and atom j in direction β. In Eq. (5), when replacing L and R with two molecule indexes, i.e., summing atomic heat flux $q_{i\to j}(\omega)$ over the atoms that belong to two molecules, one can also obtain the spectral heat flux between two molecules. By integrating the spectral heat flux over frequency, the total heat flux between any pair of molecules could be obtained.

3 Results and discussions

3.1 Temperature and Pressure effects on Thermal Conductivity

To calculate the TC, we first tested the convergence against box size in Fig. Sxx. As shown in the figure, the TC does not change significantly with the sizes tested, especially after ~4.5 nm. As a result, all TC is calculated with the box size of ~4.5 nm. The top panel of Fig. 1 illustrates the two molecules that we studied, namely TPD and mCP, both of them contain soft dihedral bonds. The morphology of amorphous TPD and mCP is illustrated in Fig. Sxx. Fig. 1(a) shows the temperature dependent TC computed using both the full expression of the heat flux, including the

Commented [DD1]: Reference

Commented [DD2]: Reference

convective contribution, and only the Virial part of the heat flux. It reveals that the TC calculated based on the total heat flux is significantly larger than that based on only the Virial contribution for both molecules in the considered temperature range. The difference ranges from 0.2 to 0.4 $Wm^{-1}K^{-1}$, depending on the molecule and temperature, that is up to 25% of the total TC. The difference arises from both the autocorrelation part of the convective heat flux and the cross-correlation between the convective and the Virial currents (Fig. S3 and Table S3). As a result, we argue that it is essential to include convective heat flux when studying thermal transport in soft low TC materials. Interestingly, the TC dependence to temperature is stronger when the kinetic part is involved (solid lines). Without considering the kinetic contribution, the TC (dash lines) is almost temperature independent. It is worth highlighting that our simulated TC is larger than the measured one[11], which might be due to the following reasons: (i), the inaccuracy of the empirical potential; (ii), the relatively small simulation box we used, which can lead to quasi periodicity for the systems; (iii), the morphology difference between experimental and simulation structure. As the main goal in this work is to study thermal transport mechanisms in amorphous organic materials as well as the temperature and pressure effect on TC, the absolute value of TC is not essential and will not change the TC trends and our conclusions. Hereafter we will only discuss TC calculated including the convective flux.

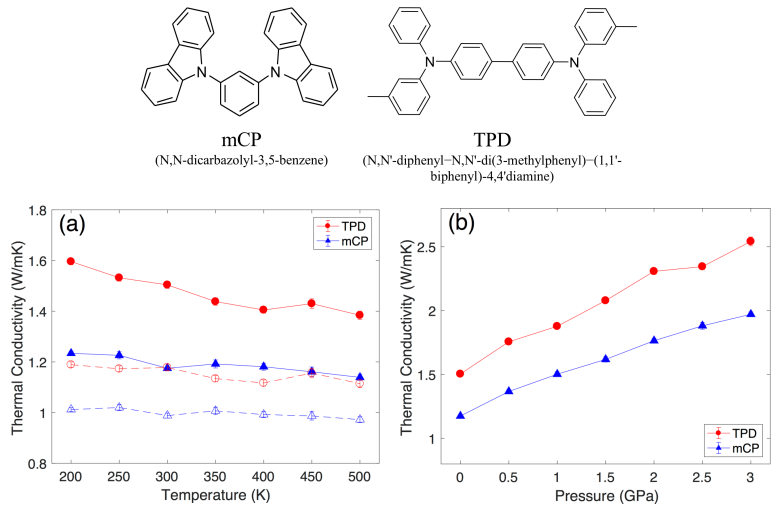

Fig. 1. The molecular structures of mCP and TPD (up panel). (a) Temperature dependent thermal conductivity of TPD and mCP with (solid lines) and without (dash lines) the contribution from the convective heat flux; (b) Pressure dependent thermal conductivity of TPD and mCP at 300 K. The error bars are determined by the standard error and some of the error bars are smaller than the symbol size.

Since the interatomic interactions between organic molecules are much weaker than those in inorganic systems, organic materials can be easily compressed. To study the pressure effect on thermal transport in the four systems, we calculated their TC under different pressures up to 3 GPa at 300 K as shown in Fig. 1(b). The TC of both molecules substantially increases with pressure by

up to 90% and 70% at 3 GPa for mCP and TPD, respectively. In the pressure range we studied, pressure increase the TC of both molecules linearly. With the compression of the systems, the interaction between molecules becomes stronger, thus facilitating energy transport among molecules and leading to an increased TC.

3.2 Vibrational Density of States

To characterize the pressure effect on TC, we calculated the vibrational density of states (VDOS) based on the atomic velocities (Eq. 2). Fig. 2 illustrates the VDOS of the two molecule systems at different pressures. For both structures, the low frequency VDOS is reduced with the increase of pressure. Especially when the pressure increases from 0 to 1 GPa, where the DOS below 1 THz is reduced noticeably. With the further increase of pressure to 3 GPa, the DOS below 1 THz continue to reduce but with a smaller speed. Accompany with the reduction of DOS at low frequencies, the height of the first peak is also reduced and right shifted, which is associate to the strengthened molecular interactions at high pressure. Although there is no well-defined wave vector in amorphous materials, the low frequency modes can still travel as acoustic waves with fairly long mean free paths, i.e., behaving as phonons. Previous studies in amorphous inorganic materials reveal that the total TC can be divided into the contributions by propagating modes at low frequencies and *"diffusons"* at high frequencies[21-23]. This conclusion is also valid in amorphous organic materials as will be demonstrated by our mode relaxation time analysis. It is then reasonable to hypothesize that the enhanced interactions between molecules at high pressures stiffens the acoustic phonon and upshifts the frequencies, thus increasing the phonon group velocities, which is evidenced by the pressure dependent sound velocities reported in Table S3. Consequently, the low frequency VDOS will be reduced and red shifted with the increase of pressure. The enhanced phonon group velocity at low frequency eventually leads to the observed increase of TC with pressure.

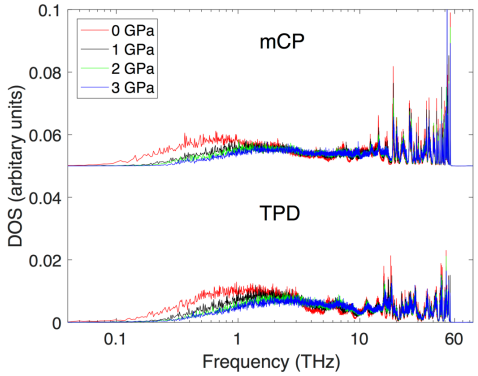

Fig. 2. Vibrational density of states (VDOS) of mCP and TPD at 0, 1, 2, and 3 GPa. The VDOS of mCP is upshifted by 0.05.

3.3 Mode diffusivity

As discussed above, the modes at intermediate and high frequencies in amorphous materials are delocalized but do not have well-defined polarization and cannot properly be characterized by group velocities. They transfer energy via a hopping mechanism between modes of similar frequency, which are defined *diffusons*. Diffusons, while not propagating as phonons in crystals,

are spatially delocalized and can carry heat through a hopping mechanism among modes with similar frequency. This mechanism contributes the most to heat transport in disordered systems[18, 23, 24]. The delocalization of vibrational modes over neighboring molecules can be evidenced by the participation ratio as shown in Fig. S4, where the modes below 10 THz can reach up to 0.3. To quantify the relative contributions from propagating phonons and diffusons in amorphous organic materials, we apply the Allen-Feldman model[18] to calculate the mode diffusivity. The diffuson TC can be casted from the diffusivity based on Eq. (3-4). Fig. 3(a) shows the mode diffusivity at 0 GPa of TPD and mCP. In general, the diffusivity of both structures decreases with the increase of frequency. The diffusivity below 1.0 THz follows a frequency dependence as ω^{-3}, which may possibly arise from the combination of anharmonic scattering (ω^{-2})[25-27] and amorphous/point defect scattering (ω^{-4})[21, 27, 28]. For both mCP and TPD, the integrated TC based on the diffusivity is smaller than that obtained from MD simulations (Fig. 3(b)), which reveals that the contribution from the low frequency propagating modes cannot be neglected. Since the propagating modes have MFP much larger than that of diffusons, using diffusivity will underestimate the TC at low frequencies. From **Fig. 3(b)** we deduce that the modes above 10 THz almost do not contribute to the total TC in both molecules due to their low mode diffusivity, which is also revealed by our spectral heat current calculations as will be discussed later.

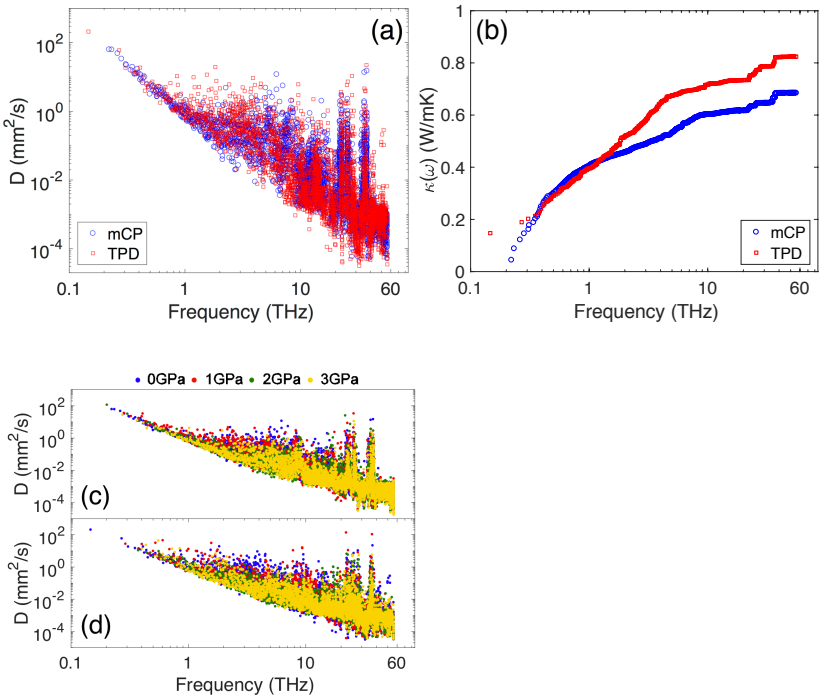

Fig. 3. (a) Mode diffusivity of TPD and mCP under 0 GPa; (b) accumulative thermal conductivity based on mode diffusivity at 300K and 0 GPa; (c)-(d) mode diffusivity at 0, 1, 2, and 3 Gpa for mCP (c) and TPD (d).

To achieve a deeper understanding of how TC changes with pressure, we also calculated the mode diffusivity of the two molecular systems under different pressures. Fig. 3(c) demonstrates the mode diffusivity under 0, 1, 2, and 3 GPa for the two molecule systems. With the increase of pressure, the distribution range of mode diffusivity is narrowed at all frequencies. On the one hand, at low frequencies, the frequency range, where diffusivity scales as ω^{-3}, is extended. On the other hand, the mode group velocities are enhanced by pressure (Table. S1), especially at low frequencies. Consequently, there are more modes with mean free path larger than the wavelength. Both the extension of ω^{-3} for diffusivity and increased mode mean free path indicate that some of the modes can convert from diffusons to propagons under pressure, thus carrying more thermal energy and eventually leads to a large enhancement of TC with the increase of pressure. At 3 GPa, the ω^{-3} range for both structures is extended to 1.5 THz.

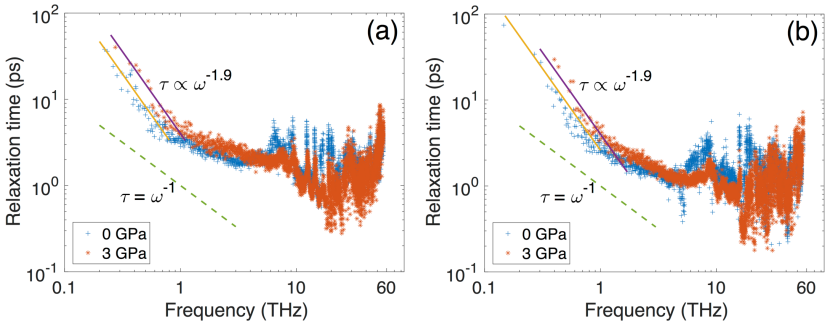

Fig. 4 Mode relaxation time of mCP (a) and TPD (b) under 0 GPa and 3 GPa.

3.4 Mode relaxation time

The AF diffusivity can give a quantitative estimation of the high-frequency modes, i.e., diffusons. While for the low frequency modes, they can propagate longer than their wavelength, thus can not be characterized by diffusivity. To illustrate the behavior of those modes, we perform the spectral energy density (SED) calculations and extract the mode relaxation times from SED. Fig. 4 demonstrates the obtained mode relaxation time of mCP and TPD under 0 and 3 GPa. In general, the relaxation time of both structures decreases with the increase of frequency. At low frequencies, the relaxation time under 0 and 3 GPa is roughly in proportional to $\omega^{-1.9}$, which is close to the phonon anharmonic scattering ω^{-2} found in amorphous Silicon[21, 29]. The relaxation time of those modes is also larger than the Ioffe-Regel limit [30, 31], i.e., ω^{-1}. Both phenomena indicate that the low frequency modes behavior as propagon. With the increase of pressure, the relaxation time at low frequencies of both structures is enhanced. As a result, it will increase the contribution of low frequency propagons to the total TC, which is one reason that leads to the fast increase of TC under pressure. Similar to the ω^{-3} scaling of diffusivity under pressure, the frequency range of relaxation time at low frequencies ($\omega^{-1.9}$) is also extended. For mCP, the frequency range of $\tau \propto \omega^{-1.9}$ is extended from 0.8-1.0 THz at 0 GPa to 1.2-1.5 THz at 3 GPa. While for TPD, the corresponding frequency is 1.0-1.2 THz and 1.7-2.0 THz under 0 and 3 GPa, respectively. The extension of $\omega^{-1.9}$ scaling of relaxation time under pressure indicates that pressure can convert diffusons to propagons, which can also lead to the increase of TC. In crystalline materials,

pressure can enhance the phonon group velocity but also break lattice symmetry [32, 33]. The break of lattice symmetry can enhance the anharmonic phonon scattering and thus compete with the phonon group velocity, making the pressure effect on TC more complicated. However, in amorphous organic materials, pressure promotes thermal transport by enhancing the low frequency phonon group velocity and relaxation time, and simultaneously changing the vibrational modes from diffuson to propagon. That is why pressure can enhance the thermal transport noticeably in organic materials.

Beyond the $\omega^{-1.9}$ scaling trend, the relaxation time decrease slower and the scaling changes to approximately $\omega^{-0.3}$ for mCP and $\omega^{-0.6}$ for TPD. Beyond 10 THz, the relaxation time spans between less then 1 ps to a few picoseconds for both structures. It is worth to note that pressure only enhances the relaxation time below a few THz. The relaxation time at high frequencies will not be affected and even be reduced at middle frequency range for both molecular systems as indicated by Fig. 4.

3.5 Spectrally decomposed heat flux

To further characterize the mode dependent properties, especially the low frequency mode contribution to the thermal transport, we perform non-equilibrium molecular dynamics (NEMD) simulations and calculated the spectrally decomposed heat flux for all systems. In the NEMD process, firstly we generate a well-relaxed structure of ~4×4×17.6 (nm) in dimension for each material. The Langevin thermal bath was applied to establish the non-equilibrium steady state with the coupling constant of 1 ps. The heat baths are 7 nm thick along the z direction and the temperature difference between the heat source and heat sink was set to 60 K. After the system reached non-equilibrium steady state, we calculated the spectrally decomposed heat flux according to Eq. 5-6. It should be noted that to save computational costs, we have used relatively small systems, which allows us to make qualitative analysis on the relative contribution for the modes of different frequencies. **Fig. 5** shows the frequency resolved heat flux of TPD and mCP at 300 K. For both structures, the heat flux beyond 10 THz is very small, which is in agreement with our accumulative TC evaluated from the mode diffusivity. Below 1 THz, the heat flux is relatively large, indicating the contribution of phonons is important, which is also consistent with our diffusivity analysis.

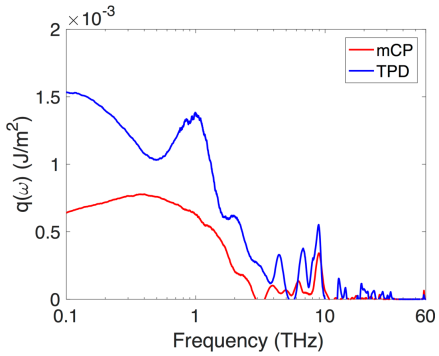

Fig. 5. Spectrally decomposed heat flux of mCP and TPD. Insert: the zoom in plot of the spectrally decomposed heat flux below 5 THz.

Since intramolecular bonds are covalent, energy is transferred very efficiently (ballistic transport) within the molecule, so the overall thermal conductivity in (amorphous) organic materials is controlled by intermolecular interactions. To get the details of heat transfer among molecule pairs, we calculated the heat flux between individual molecule pairs that connect an imaged interface (locate at the right middle of the system). The centroid of each molecule is used to determine its location, i.e., the molecules whose center of mass is located on the left/right side of the interface are defined as the left/right molecule. We summed the heat flux of all pairs of atoms associate to the molecule pairs to obtain the heat flux of each pair of molecules (see Methods) and the results are demonstrated in **Fig. 6**. In general, the heat flux between molecules strongly depends on their distance with the heat flux decreasing rapidly with inter-molecule distance. At a fixed molecular distance, the heat flux can span two to three orders of magnitudes, which should be associate to different orientations of molecules. For both systems, the main contribution to the total heat flux comes from the molecule pairs with distances short than 1.4 nm. For large distances, the molecules mainly interact with each other through Coulomb forces, i.e., point charges, the potential of which decay with r^{-1}. Consequently, the molecule pair heat flux is rapidly reduced with the increase of their distance. We stress that the above distance of 1.4 nm refers to the molecular center-of-mass distance and this distance is already very large for Coulomb interactions. The actual heat flux should be contributed by atom pairs shorter than this distance.

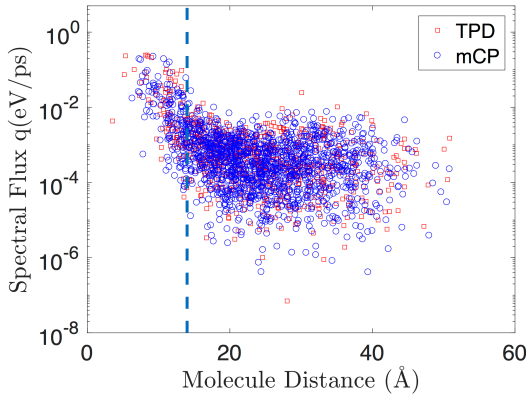

Fig. 6. Heat flux between molecular pairs separated by an interface.

4. Conclusions

Based on molecular dynamics simulations, we studied the temperature and pressure dependent thermal transport in amorphous small organic molecule systems, namely TPD and mCP. We found that in such low TC systems, the kinetic energy contribution to the total heat flux is important in Green-Kubo formula. The contribution of the kinetic heat flux in TPD can be as large as 24% at 200 K. The kinetic heat flux is also temperature dependent, which leads to the decrease of total TC

with temperature. Similar to inorganic amorphous materials, the TC in amorphous organic systems can be divided into the contributions of propagons at low frequencies and diffusons at high frequencies. The main contribution of diffusons arises from the frequencies between 10 THz, beyond which the diffuson TC is negligible due to the small diffusivities. Such a conclusion has also been revealed by spectral heat flux calculations. With the increase of pressure, the TC can be greatly enhanced in all systems due to the increase of sound velocity, relaxation time of low frequency modes and the conversion of diffusons to propagons simultaneously. As a result, the propagon contribution to the total TC under high pressure is increased greatly. Although long-range Coulomb interactions exist in both systems, the molecule pair heat flux analysis reveals that only molecule pairs with distances below 1.4 nm contribute significantly to the total heat flux. The heat flux between molecule pairs beyond 1.4 nm is orders of magnitude smaller than that below 1.4 nm. Our studies could be meaningful to the understanding of thermal transport mechanism in amorphous organic materials, which are important for the improvement of electronic device performances.

Acknowledgements

S. Xiong acknowledges the financial support from National Natural Science Foundation of China (Grant No. 11804242), and the Jiangsu Provincial Natural Science Foundation (Grant No. BK20160308).

Reference

1. Forrest, S. R., The path to ubiquitous and low-cost organic electronic appliances on plastic. *Nature* **2004,** *428*, 911.
2. Shakouri, A., Nanoscale Thermal Transport and Microrefrigerators on a Chip. *Proceedings of the IEEE* **2006,** *94* (8), 1613-1638.
3. Wang, X.; Zhang, J.; Chen, Y.; Chan, P. K., Molecular dynamics study of thermal transport in a dinaphtho [2, 3-b: 2′, 3′-f] thieno [3, 2-b] thiophene (DNTT) organic semiconductor. *Nanoscale* **2017,** *9* (6), 2262-2271.
4. Pop, E.; Mann, D.; Wang, Q.; Goodson, K.; Dai, H., Thermal conductance of an individual single-wall carbon nanotube above room temperature. *Nano letters* **2006,** *6* (1), 96-100.
5. Balandin, A. A., Thermal properties of graphene and nanostructured carbon materials. *Nature Materials* **2011,** *10*, 569.
6. Sperling, L. H., *Introduction to physical polymer science*. John Wiley & Sons: 2005.
7. Tang, N.; Peng, Z.; Guo, R.; An, M.; Chen, X.; Li, X.; Yang, N.; Zang, J., Thermal transport in soft PAAm hydrogels. *Polymers* **2017,** *9* (12), 688.
8. Shen, S.; Henry, A.; Tong, J.; Zheng, R.; Chen, G., Polyethylene nanofibres with very high thermal conductivities. *Nature nanotechnology* **2010,** *5* (4), 251.
9. Henry, A.; Chen, G., High thermal conductivity of single polyethylene chains using molecular dynamics simulations. *Physical review letters* **2008,** *101* (23), 235502.
10. Wang, D.; Tang, L.; Long, M.; Shuai, Z., Anisotropic Thermal Transport in Organic Molecular Crystals from Nonequilibrium Molecular Dynamics Simulations. *The Journal of Physical Chemistry C* **2011,** *115* (13), 5940-5946.
11. Kim, N.; Domercq, B.; Yoo, S.; Christensen, A.; Kippelen, B.; Graham, S., Thermal

transport properties of thin films of small molecule organic semiconductors. *Applied Physics Letters* **2005,** *87* (24), 241908.
12. Plimpton, S., Fast parallel algorithms for short-range molecular dynamics. *Journal of computational physics* **1995,** *117* (1), 1-19.
13. Jorgensen, W. L.; Maxwell, D. S.; Tirado-Rives, J., Development and testing of the OPLS all-atom force field on conformational energetics and properties of organic liquids. *Journal of the American Chemical Society* **1996,** *118* (45), 11225-11236.
14. Nosé, S., A unified formulation of the constant temperature molecular dynamics methods. *The Journal of Chemical Physics* **1984,** *81* (1), 511-519.
15. Green, M. S., Markoff random processes and the statistical mechanics of time‐dependent phenomena. II. Irreversible processes in fluids. *The Journal of Chemical Physics* **1954,** *22* (3), 398-413.
16. Kubo, R., R. Kubo, J. Phys. Soc. Jpn. 12, 570 (1957). *J. Phys. Soc. Jpn.* **1957,** *12*, 570.
17. Dickey, J., JM Dickey and A. Paskin, Phys. Rev. 188, 1407 (1969). *Phys. Rev.* **1969,** *188*, 1407.
18. Allen, P. B.; Feldman, J. L., Thermal conductivity of disordered harmonic solids. *Physical Review B* **1993,** *48* (17), 12581.
19. Sääskilahti, K.; Oksanen, J.; Tulkki, J.; McGaughey, A.; Volz, S., Vibrational mean free paths and thermal conductivity of amorphous silicon from non-equilibrium molecular dynamics simulations. *AIP Advances* **2016,** *6* (12), 121904.
20. Sääskilahti, K.; Oksanen, J.; Tulkki, J.; Volz, S., Role of anharmonic phonon scattering in the spectrally decomposed thermal conductance at planar interfaces. *Physical Review B* **2014,** *90* (13), 134312.
21. Larkin, J. M.; McGaughey, A. J. H., Thermal conductivity accumulation in amorphous silica and amorphous silicon. *Physical Review B* **2014,** *89* (14), 144303.
22. Donadio, D.; Galli, G., Atomistic Simulations of Heat Transport in Silicon Nanowires. *Physical Review Letters* **2009,** *102* (19), 195901.
23. Zhou, Y.; Xiong, S.; Zhang, X.; Volz, S.; Hu, M., Thermal transport crossover from crystalline to partial-crystalline partial-liquid state. *Nature Communications* **2018,** *9* (1), 4712.
24. Feldman, J. L.; Allen, P. B.; Bickham, S. R., Numerical study of low-frequency vibrations in amorphous silicon. *Physical Review B* **1999,** *59* (5), 3551-3559.
25. Callaway, J., Model for Lattice Thermal Conductivity at Low Temperatures. *Phys Rev* **1959,** *113* (4), 1046-1051.
26. Xiong, S. Y.; Selli, D.; Neogi, S.; Donadio, D., Native surface oxide turns alloyed silicon membranes into nanophononic metamaterials with ultralow thermal conductivity. *Phys Rev B* **2017,** *95* (18), 180301.
27. Holland, M. G., Analysis of Lattice Thermal Conductivity. *Phys Rev* **1963,** *132* (6), 2461-&.
28. Hondongwa, D. B.; Daly, B. C.; Norris, T. B.; Yan, B.; Yang, J.; Guha, S., Ultrasonic attenuation in amorphous silicon at 50 and 100 GHz. *Phys Rev B* **2011,** *83* (12), 121303.
29. Wingert, M. C.; Zheng, J.; Kwon, S.; Chen, R., Thermal transport in amorphous materials: a review. *Semiconductor Science and Technology* **2016,** *31* (11), 113003.
30. Taraskin, S. N.; Elliott, S. R., Determination of the Ioffe-Regel limit for vibrational excitations in disordered materials. *Philosophical Magazine B* **1999,** *79* (11-12), 1747-1754.
31. Zhu, T. S.; Ertekin, E., Generalized Debye-Peierls/Allen-Feldman model for the lattice thermal conductivity of low-dimensional and disordered materials. *Phys Rev B* **2016,** *93* (15), 155414.

32. Shao, C.; Yu, X.; Yang, N.; Yue, Y.; Bao, H., A Review of Thermal Transport in Low-Dimensional Materials Under External Perturbation: Effect of Strain, Substrate, and Clustering. *Nanoscale and Microscale Thermophysical Engineering* **2017,** *21* (4), 201-236.
33. Wan, Y.; Xiong, S.; Ouyang, B.; Niu, Z.; Ni, Y.; Zhao, Y.; Zhang, X., Thermal Transport Engineering in Graphdiyne and Graphdiyne Nanoribbons. *ACS Omega* **2019,** *4* (2), 4147-4152.